FR9401950

CRN STRASBOURG

CRN 93-09

BETA DECAY OF ^{31,32}Na AND ^{31}Mg: STUDY OF THE N = 20 SHELL CLOSURE

G. Klotz, P. Baumann, M. Bounajma, A. Huck, A. Knipper, G. Walter
Centre de Recherches Nucléaires et Université Louis Pasteur,
F-67037 Strasbourg, France

G. Marguier
Institut de Physique Nucléaire et Université Claude Bernard,
F-69622 Villeurbanne, France

C. Richard-Serre
CERN 1211 Geneva 23, Switzerland
and IN2P3, F-75013 Paris, France

A. Poves and J. Retamosa
Departamento de Fisica Teorica, C-XI, Universidad Autonoma, Cantoblanco,
E-28049 Madrid, Spain

Accepted for publication in Phys. Rev. C

CENTRE DE RECHERCHES NUCLEAIRES

STRASBOURG

IN2P3 CNRS

UNIVERSITE LOUIS PASTEUR

BETA DECAY OF ^{31,32}Na AND ^{31}Mg : STUDY OF THE N = 20 SHELL CLOSURE

G. Klotz, P. Baumann, M. Bounajma, A. Huck, A. Knipper, G. Walter
Centre de Recherches Nucléaires et Université Louis Pasteur,
F-67037 Strasbourg, France

G. Marguier
Institut de Physique Nucléaire et Université Claude Bernard,
F-69622 Villeurbanne, France

C. Richard-Serre
CERN 1211 Geneva 23, Switzerland
and IN2P3, F-75013 Paris, France

A. Poves and J. Retamosa
Departamento de Fisica Teorica, C-XI, Universidad Autonoma, Cantoblanco,
E-28049 Madrid, Spain

Abstract

The ^{31,32}Na and ^{31}Mg beta decays were studied at the CERN on-line mass separator ISOLDE by gamma, gamma-gamma and neutron-gamma measurements. In the ^{31}Na decay, the assignment of previously reported γ transitions and the observation of a new level at 3760 keV lead to a revised decay scheme which is found in good agreement with a calculation including 2p-2h configurations in the model space, as far as only low-lying levels of ^{31}Mg are concerned. In the ^{31}Mg → ^{31}Al decay, a new decay scheme involves ten β branches and three states are reported for the first time. While satisfactory agreement with theoretical calculations is observed for excitation energies in ^{31}Al, a strong discrepancy is observed for the intensity of the ground state β branch, the experimental one being highly quenched as compared to theoretical expectations. Finally, new spectroscopic results have been obtained in the ^{32}Na β^- decay. A previously non-interpreted 1436 keV γ ray is now assigned in the ^{32}Mg scheme. The 240 keV ray is shown to arise from ^{31}Mg produced in the one-neutron channel, and to be related to the decay of an intruder state at E_x = 461 keV. The latter is partially fed from the 1390 keV level. Both nicely compare with theoretical predictions locating $1\hbar\omega$ states at 0.40 MeV ($7/2^-$) and 1.57 MeV ($11/2^-$). The first experimental evidence for a γ cascade in the descendant ^{32}Al is also obtained.

I. INTRODUCTION

Studies of neutron-rich nuclei in the region around Z=11, N=20 have been initiated by the mass measurements of Na and Mg isotopes [1,2], indicating an excess in binding energy, and stimulated by the subsequent observation of a low lying excited state in the even-even ^{32}Mg isotope [3].

The experimental evidences for a region of strong deformation along a single closed shell have been documented since then by additional results on neighboring nuclei and detailed comparisons with theoretical descriptions. When compared to shell model calculations, very successful for the N=18 isotones, the N=20 nuclei ^{31}Na and ^{32}Mg appeared incompatible with a shell model description [4]. Likewise, the ^{31}Mg spectrum was found completely anomalous in the context of sd-shell systematics among the N=19 isotones [5]. A better agreement with the experimental results was obtained by Hartree-Fock calculations on Na isotopes with contribution of the f7/2 orbit for the neutron [6] and by shell model calculations in the (sd,f) [7] or (sd,fp) [8] space.

The importance of the $(sd)^{-2}(fp)^{2}$ neutron configurations in the low energy states of N=20 isotones was confirmed by the observation of the ^{34}Si level scheme and its shell model interpretation with a mixed $(0+2)\hbar\omega$ calculation [9].

Detailed discussions of the mechanisms responsible for the lowering of the $2\hbar\omega$ excitation relative to $0\hbar\omega$ and leading to a region of inversion around ^{32}Na have been published recently [10,11,12]. In the study by Warburton et al.[10], calculations are made separately for the $0\hbar\omega$ and $2\hbar\omega$ excitations, the results of a weak coupling model being used to relate the excitation energy of the $n\hbar\omega$ configurations to the calculated $0\hbar\omega$ binding energies. A good predictive power is obtained for binding energies of N ≥ 20 nuclei apart from the fact that ^{32,33}Na remain still underbound. When compared to the results of the mixed $(0+2)\hbar\omega$ calculations [11,12], a general agreement is found with differences in the properties of excited states of N=19 and N=20 isotopes.

The existence of a deformed region, with coexisting spherical and deformed states at low energy for ^{31}Na, ^{32}Mg, ^{33}Al and ^{34}Si has also been suggested by Heyde and Wood [13] using methods already applied to the evaluation of 2p-2h intruder excitations along single-closed shells in different places of the nuclear mass table [14]. More recently the strong deformation of several neutron rich Na and Mg isotopes has been predicted by Patra and Praharaj [15] using a relativistic mean field model of interacting nucleons and mesons.

The experimental information on binding energies in the region around Z=11, N=20, is now well documented with new mass determinations [16,17,18,19]. On the contrary, the knowledge of excited states of N=19, 20 nuclei from previous β-decay [20] and multi-nucleon transfer reaction [21,22,23] studies is far from complete. More experimental data are needed in order to delineate the region of $0\hbar\omega$ and $2\hbar\omega$ inversion, locate the energies of intruder states and extend the comparison with the calculations.

The present investigation of the ^{31}Na decay was therefore undertaken to study the ^{31}Mg isotope (N=19) which provides an interesting case for testing the predictions of models relative to $0\hbar\omega$ and $1\hbar\omega$ excitations. A return to the ^{32}Na decay was also necessary because of the importance of the ^{32}Mg level structure for the understanding of this region and the possibility to populate specific levels in ^{31}Mg through the beta-delayed 1n channel. To sort out experimental data, a reinvestigation of the β decay of ^{31}Mg was necessary and it allowed to add spectroscopic information in the ^{31}Al level scheme. This information is particularly valuable as the ^{31}Al low energy level scheme is perfectly reproduced in sd-shell model calculations and contradictions for upper levels can reveal an anomaly in the N=20 shell closure. Preliminary results have been reported in Ref. [24].

The experimental conditions are first briefly described. The results obtained in the beta decay studies of ^{31}Na, ^{31}Mg and ^{32}Na are then presented. The shell model calculations and the theoretical predictions which can be compared to the measurements are discussed.

II. EXPERIMENTAL METHODS

In our experiments, Na, Mg and Al isotopes were produced by bombarding an uranium carbide target ($\approx$ 15 g/cm^2) with 2.0 μA 600 MeV protons from the CERN synchrocyclotron. These different atoms were ionized through surface ionization and mass separated in the ISOLDE 2 separator. Typical yields for ^{31}Na ($T_{1/2}$= 17 ms) and ^{32}Na ($T_{1/2}$= 14 ms) were 100 and 15 atoms/s respectively. Magnesium and aluminium isotopes resulted either from radioactive decay or direct production from the source. In spite of the higher ionization potential and the lower volatility of these elements, their direct production from the target is observed when the ion source temperature is increased and this feature has been turned to account in previous studies [9,25].

The selected beams were collected on a moving tape system where suitable collection-counting cycles were chosen to optimize the observation. The set-up included a thin NE102 plastic scintillator for beta detection (80 % efficiency) at the collection point, two germanium gamma counters and an efficient neutron detector consisting of three hexagonal cells each filled with 3750 cm^3 NE 213 liquid scintillator. This set-up allowed to perform β-γ, β-γ-γ and β-γ-n measurements and multiparametric events were registered on magnetic tape for subsequent analysis. A small BaF_2 counter was also used to measure the lifetime of low-energy transitions.

III. EXPERIMENTAL RESULTS

A - The experimental β^- decay of ^{31}Na

Before the present work, information on the β decay of ^{31}Na resulted from Ref. [20] and the therein quoted studies. From these investigations, we use the following important parameters : (i) the half-life of 17.0 $\pm$ 0.4 ms ; (ii) the P_{1n} and P_{2n} values, 37.3 $\pm$ 5.4 and 0.87 $\pm$ 0.24 respectively.

The estimated Q_β value of 15.42 $\pm$ 0.51 MeV is a computed weighted average deduced from the mass excesses of ^{31}Na and ^{31}Mg given in a compilation [26] and in recent measurements at GANIL [18] and Los Alamos [19]. Although the origin

of this parameter is different from that of the corresponding one in Ref. [20], the inferred result comes out at nearly the same value. The updated mass value Q_β is also used to calculate the one- and two-neutron separation energies in ^{31}Mg locating as a result the ^{29}Mg and ^{30}Mg excited level systems relatively to the ^{31}Mg ground state. These are fed in the β-delayed one and two neutron processes.

The energy and the intensity of the γ rays observed in the β decay of ^{31}Na are listed in Table I. The γ-branching ratios in ^{31}Mg are given in Table II. It is noteworthy that two weak γ rays arising in the deexcitation of ^{29}Mg are observed. Only an upper limit on their intensity was given previously. Their actual detection is a definite argument in favour of a non-vanishing value of the β-delayed two-neutron probability in the β decay of ^{31}Na.

1. Level scheme of ^{31}Mg resulting from the 0-n process

The disintegration scheme of ^{31}Na ($J^\pi = 3/2^+$, Refs. [27,8]) is shown in Fig.1. In comparison with the results of Ref. [20] and on the basis of our coincidence data, one level at 895 keV is invalidated. On the other hand, four previously unreported states are added to the excitation scheme of the final nucleus.

The β intensity to the ground state of ^{31}Mg is calculated assuming the P_n values of Ref. [28] and the absolute γ intensities as determined according to our decay scheme. Since several parameters affected by uncertainties occur in series in this calculation, the final value is not very precise. Nevertheless our result is comparable with the one given in Ref. [20], although somewhat smaller, which leads, but not sufficiently, to a more satisfactory agreement with theory as will be seen in section IV.

Care was taken in this work to get reliable efficiency curves of the germanium detectors, even at very low energy. An estimate of the γ intensity balance of the first excited state at 50 keV, and consequently of its β feeding, can then be given. As a result, it was possible to bring into relief the strong difference between the β_0 and the β_1 branch intensities.

The 50 keV level was found to be relatively long-lived. The measurement of its half-life was carried out by means of the observation of coincidences between fast signals corresponding to the β detection in a 3π plastic scintillator surrounding the ^{31}Na sources and γ detection in a BaF_2 crystal (36 mm in diameter, 6 mm thick) viewed by a XP 2020 Q phototube. This latter device is known to exhibit excellent timing properties along with a sufficiently good resolution power at low energy, typically 20 keV FWHM at 60 keV as measured with a ^{241}Am standard. The biparametric spectrum obtained by storing the energy signals versus the time to amplitude converter response between the two detectors is shown in Fig.2. The only delayed events correspond to the deexcitation of the 50 keV level. A conventional representation of its decay is displayed in the insert. The deduced half-life $T_{1/2}$ is equal to 16.0 ± 2.8 ns.

The β intensity to the second excited state at 221 keV appears now to be very low. Only an upper limit of 2.2 % can be inferred from the γ imbalance in contrast with Ref. [20] where an actual branch of 5.4 % was assumed. The corresponding log ft value differs by at least one unit.

We establish a new level at 673 keV, substantially populated according to our results. The evidence for the 673 keV γ ray to deexcite a level of the same energy towards the ground state in competition with the 623 keV γ ray going to the first excited 50 keV state discussed above was not considered previously, as a 623 keV line occurs alike as a transition in the descendant ^{31}Al β decay (2316.8 to 1695.0 keV in ^{31}Si). The existence of a doublet is necessary to explain the whole observed intensity of the 623 keV line. This assignment is supported by the γ-γ measurements : Fig.3 shows clearly a 623 keV line in coincidence with a 50 keV one. A further and conclusive argument is the presence of a 452 keV line coincident with the 50, 171 and 221 keV lines as displayed in Fig.4. This ray corresponds to an additional decay mode of the 673 keV level. It is not easily detectable in the direct spectrum, being located close to the right edge of a strong line at 444 keV due to the descendant (688.1 to 244.3 keV in ^{30}Al).

Fig.3 illustrates another new result. It clearly appears there that the 895 keV line originating in the deexcitation of ^{31}Na should not be attributed to a transition to the ground state but to the first excited state at 50 keV, which is a firm signature for a new level at 945 keV.

Going on upwards, the levels at 1029 and 2243 keV are confirmed. In the case of the β branch intensity to the first one, we are only able to secure an upper limit, which is not in contradiction however with the known results.

Finally, we locate two new levels at 3760 and 3814 keV on the basis of γ-γ measurements. Strong electromagnetic deexcitation modes of states situated above the neutron separation energy were already encountered in previous works, in this mass region, in particular in ^{48,49}K β-decay studies [29] .

2. The β-delayed neutron emissions from ^{31}Na

The absolute intensities of the neutron feeding of 6 levels in ^{30}Mg including the ground state are listed in Table V. Normalization is obtained via γ-ray intensities compared to those noticed in the ^{31}Na (β^-) ^{31}Mg process. The total of the neutron branches towards the ground state is taken as the difference between the P_n value [28] and the normalized strength populating the excited levels. No additional states, in comparison with those reported [20], are observed.

In a similar way, we inferred the corresponding quantities for the 2n process. The detection of two γ rays at 1040 and 1638 keV gives evidence of a weak neutron strength to levels at 1095 and 1638 keV in ^{29}Mg. (Table I and Fig.1). The existence of the 55 keV line is known from a previous work [30]. It cannot be observed in the present work, being masked by the strong deexcitation peak of the first level in ^{31}Mg at almost the same energy. Therefore it was not possible to estimate the amount of neutron strength implying separately each member of the ^{29}Mg ground state doublet.

B - The experimental β^- decay of ^{31}Mg

Like in the case of ^{31}Na, the half-life of 250 ± 30 ms, as well as the P_{1n} value were taken from Ref. [28]. A new estimate for the Q_β value was computed with the help of data published in Refs. [16,17,26]. Yet again the obtained result of 11.69 ± 0.27 MeV is not significantly different from 11.42 MeV adopted previously. The neutron separation energy S_n originates from the same sources.

The γ rays attributed to transitions in the ^{31}Al nucleus are listed in Table VI along with their intensity and assignment. They are similar to those of Ref. [20], however the assignment of all lines could now be established.

In Table VII are shown the γ branching ratios as inferred from our measurement. Table VIII gives the β branching and the corresponding log ft values.

The level scheme of ^{31}Al established in this work and displayed in Fig.6 contains several new results important for the description of the low energy structure of ^{31}Al. The most interesting one is the suppression of a state at 2530 keV assumed to arise from the decay of a 3434 keV level through a 904 keV line [20]. It is easy to rule out this assertion on account of our coincidence data (Figs.7,8). The two lines (904, 2530 keV) are well interpreted if one considers the existence of a new state at 4143 keV, which they deexcite. According to observed coincidences, this state is besides connected with the 3196 keV line formerly assumed to be emitted from the 4809 keV level. An additional argument in this sense is shown in Fig.8 where a strong lack for the 666 keV (1613 to 947 keV) line intensity is observed compared to the 947 keV one.

At higher energy, we locate a new state at 4562 keV revealed by 2949-666-947 coincidences. Finally another new level, involving 4201-947 coincidences is placed at 5148 keV.

As no appreciable γ strength in ^{31}Al remains now unexplained, we can deduce the β_0 intensity value of 12.9 ± 6.0 from the absolute γ intensities. Due to the faintness of the β-delayed neutron channel (P_n = 1.7 ± 0.3, Ref. [28]) no reasonable possibility of observing γ lines from ^{30}Al is expected.

C - The experimental β^- decay of ^{32}Na

The β^- decay of ^{32}Na was studied with the same techniques as in the case of mass 31. However, the experimental conditions were less favourable on account of the following points : i) a weaker production yield ($\leq$ 15 atoms/s) due to the increased remoteness from stability ; ii) the disturbing presence of ^{32}Al directly produced but not separated from the isobar ^{32}Na by the mass spectrometer, competing with the part arising in the radioactive filiation ; iii) a cumbersome background resulting from the A=128 chain corresponding to multicharged ions (mainly ^{128}In and its descendants, A = 4 x 32, q = 4$^+$) neither eliminated by the separator.

The γ-ray energies and intensities observed in and attributed to the decay of ^{32}Na are listed in Table IX. In our experiment, no attempt was made to yield high precision on γ-ray energy values since during the early stage of analysis a fair agreement with the published values was noted. The intensity of peaks perturbed by contaminating lines is taken from Ref. [20]. The present value for the 1973 keV line is estimated from coincidence data. In the single spectra it is completely overwhelmed by a strong line of the same energy arising in the ^{128}In decay. The proposed decay scheme of ^{32}Na is shown in Fig.9. Half-life values are taken from Ref. [28]. Neutron separation energies are inferred from mass systematics [26]. The ^{32}Na Q_β value is revised in comparison [28], taking into account the recent mass excess measurements of Refs. [18,19] for ^{32}Mg.

The disintegration of ^{32}Na splits up into three channels where the P_{1n} and P_{2n} probabilities quoted in Ref. [20] are carried. From crude shell model considerations the ^{32}Na (Z=11, N=21) ground state has negative parity. Hence allowed β transitions can feed only negative parity states (bound or unbound) in ^{32}Mg.

The knowledge of the pure (β,γ) process, to the exclusion of beta delayed neutron channels, feeding levels in ^{32}Mg, the most deformed nucleus known in the mass region, gains some substance in comparison with the previous scheme. Three additional states are located at low energy (2117, 2321 and 2551 keV) on the basis of γ-γ coincidences involving the first excited level for the two former ones (Fig.10). As for the latter at 2.55 MeV, the non-observation of any coincidence relation leads us to

conclude in favour of a ground state deexcitation of this level. So three out of four γ rays emitted by the ^{32}Mg nucleus unexplained prior to this work, are assigned. The only non-interpreted one lies at 694 keV which seems too low to correspond to a level at this energy; on the other hand, no indication is obtained on a hypothetical cascading process implying another known level. Nevertheless, according to Table IX, this lack amounts to an almost negligible part of the whole γ strength. Absolute beta intensities deduced from gamma imbalances are given in Table X along with the corresponding log ft values. We note that all the observed β transitions have an allowed character hence populate negative parity states in ^{32}Mg. No perceptible direct β feeding of the ground and 885 keV states can take place since they are of positive parity. The absolute arithmetic γ imbalance of the 885 keV level is equal to -0.7 ± 9.8, which is compatible with a vanishing value.

The knowledge of the beta-delayed one-neutron channel is improved alike. A 240 keV γ ray previously attributed to ^{32}Mg [20], but not placed in the scheme, is clearly detected in coincidence with neutrons and with the deexciting rays of the two first states of ^{31}Mg (Figs.11,12). So it appears to be emitted in all probability by a state located at 461 keV. It is additionally in coincidence with a weak 929 keV γ ray not listed until now, which contributes to the feeding of a 461 keV level from a new state situated at 1390 keV.

A severe discrepancy between the intensity of the 240 keV ray given in Ref. [20] ($I_{abs}=16.6\pm3.2$) and in the present work ($I_{abs}=5.9\pm1.0$) remains unexplained, the former one being basically inconsistent with the new scheme. One also should notice the enhanced intensities, nearly by a factor 2, of the lines deexciting the 221 keV level. A quantitative measurement of the 50 keV γ ray could not be undertaken, due to its closeness to the detection threshold. Nevertheless, its existence is clearly observed.

In neutron emissions the lowest multipole order is favoured (usually $l = 0$), so delayed neutrons feed most likely negative parity states in ^{31}Mg. So the observed γ cascade should imply three negative parity levels : 1390 keV (π = -) → 461 keV (π = -) → 221 keV (π = -) → 50 keV (π = +). Clearly such states could not be populated in

the ^{31}Na ($J^{\pi} = 3/2^{+}$) $\beta^{-}\gamma$ process. The theoretical part of this paper (see section IV) discloses the intruder character of the negative parity states.

The neutron branching ratios for the β-delayed one- and two-neutron emissions are listed in Table XI. Due to their positive parity, the ground and the first excited states of ^{31}Mg are not expected to be substantially fed by neutron branches.

In the delayed 2n-branch an overall parity change is observed from ^{32}Na ($\pi = -$) to the ground and 2^{+} states of ^{30}Mg. This seems difficult to interpret with a di-neutron (S=0) emission, while it could be quite normal in sequential emission with different l values ($l = 0$ and $l = 1$).

D - The β^{-} decay of ^{32}Mg

Literature data [20] on this process are very scarce. The three previously reported lines (735, 2467 and 2765 keV) are confirmed in our direct spectrum. A valuable information has been obtained in our γ-γ experiment where a coincidence relationship between the 735 and 2467 keV γ rays is observed as shown in Fig.10. The weaker intensity of the latter one in agreement with results quoted in Ref. [20] means that a 735 keV level could be the intermediate state of the γ cascade (3202 keV → 735 keV → 0).

E - Extraction of some spin-parity assignments

A detailed comparison of the experimental level structure of ^{31}Al populated either by β decay or by heavy-ion transfer reactions, to sd-shell model calculations, has been discussed by Woods et al. [21]. The new data confirm the agreement for the energies and γ transitions of the first three states whose theoretical spin and energy values are $5/2^{+}$ (g.s.), $1/2^{+}$ (944 keV) and $3/2^{+}$ (1744 keV). The suppression of the 2530 keV experimental level improves the analogy at higher energies, but the electromagnetic properties are poorly reproduced by these calculations.

1. States in ^{31}Mg

The observed allowed character of β_0 and β_2 transitions in the ^{31}Mg → ^{31}Al β decay gives strong support to a limitation $J^{\pi} = (3/2, 5/2)^{+}$ of the spin and parity values of the ^{31}Mg g.s.. The $5/2^{+}$ assignment is ruled out by the log f_1t (8.4) of the β_1 transition if $J^{\pi} = 1/2^{+}$ is assumed for the 947 keV state, a second-forbidden non-unique transition would amount, at most, to a $1.5\ 10^{-4}$ β branch.

In the comparison made in Ref. [21] the experimental β_0 intensity shows a severe reduction which will be discussed in section IV. The ^{31}Na (J=3/2) → ^{31}Mg allowed β_0 transition introduces similarly a limitation for the spin value of ^{31}Mg g.s., J = (1/2, 3/2, 5/2), the values 1/2 and 5/2 being rejected above.

The measured half-life (section III.A.1) of the first excited state in ^{31}Mg limits the multipole order of the 50 keV transition to dipole. The corresponding retardation factors are $\tau/\tau_w = (3.4 \pm 0.6) \times 10^{-4}$ W.u. for E1 and $(1.1 \pm 0.2) \times 10^{-2}$ W.u. for M1 transitions. The non-observation of measurable half-life for higher levels (Fig.2) limits the multipolarity of the 221 and 171 keV transitions to L=1. An L=2 multipolarity is excluded for the two transitions as it would correspond to an unlikely value for the E2 transition strength (> 40 W.u. for the 221 KeV transition). The limit of the multipolarity sets a restriction to the spin of the 221 keV state. These limits are reported on Fig.1 using also the results of the theoretical discussion (section IV).

Among the excited states of ^{31}Mg populated from ^{31}Na via allowed β transitions, the two unbound levels at 3760 and 3814 keV ($J^{\pi} = 1/2^{+}$-$5/2^{+}$) are observed to decay by γ emission. The $J^{\pi} = 1/2^{+}$ value can be eliminated for these two levels as it would give rise to $l = 0$ neutron emission dominating the process.

The five excited states of ^{30}Mg populated in the ^{31}Na ($J^{\pi} = 3/2^{+}$) β-1 channel, also have been observed previously in the ^{30}Na ($J^{\pi} = 2^{+}$) study [30]. This situation is a particular case which will not be encountered in the ^{32}Na decay discussed below.

The ^{31}Na β-2n process populates positive and negative parity states in ^{29}Mg. This feature is similar to the one noted and discussed above for the ^{32}Na β-2n decay.

2. *Consequences for the ^{32}Na ground state*

An interesting finding of this work is a selective population of new states related by a γ cascade [E_x (^{31}Mg) : 461 and 1390 keV] through the β-1n decay of ^{32}Na. The non-observation of these levels in the ^{31}Na β decay suggests the presence of a set of levels in ^{31}Mg either of negative parity or of high spin value. This latter assumption is incompatible with their low multipolarity γ decay. The difference of ^{31}Mg states populated in the two processes may thus result from a different parity of the parent states : ^{31}Na ($J^{\pi} = 3/2^{+}$), ^{32}Na (π = -) .This interpretation is similar to the prediction of the parity of ^{32}Na by a simple shell model corresponding to a $0\hbar\omega$(1fp) or $2\hbar\omega$(3fp) g.s. configuration. A negative parity of ^{32}Na would also explain the absence of β_0 and β_1 branches in the ^{32}Na decay. The discussion relative to the 2^{+} assignment to the 885 keV level made in Ref. [20] is substantiated by our work. From the present experiment, seven excited ^{32}Mg states are now reported in the ^{32}Na decay. For all except one the deexcitation takes place through a γ cascade involving the 885 keV (2^{+}) state. The 2551 keV level populated by an allowed β transition is observed to decay only to the ground state. This allows to set an upper limit on the spin of the ^{32}Na g.s.: from our β-γ measurement the 2.55 MeV state has a half-life lower than 100 ns limiting the multipole order of the g.s. γ transition to dipole, quadrupole or E3. Hence the spin of this level is $J \leq 3$. The allowed character of the β feeding (log ft = 5.4) of this level imposes no parity change and limits the ^{32}Na g.s. spin value to $J \leq 4$.

Among the known treatments of nuclei in this region, the calculation by Warburton et al. [10] considers different possible interpretations for ^{32}Na g.s. implying either negative parity (in the case of $0\hbar\omega$(1fp), $J^{\pi} = 2^{-}$ to 6^{-}, and $2\hbar\omega$(3fp), $J^{\pi} = 0^{-}$, configurations) or positive parity with low spin value, $J^{\pi} = 0^{+}$, resulting from a coupling in a $1\hbar\omega$(2fp) configuration.

From this experiment it is difficult to assess a definite value to the ground state. Nevertheless with our results obtained in the β-1n ^{32}Na study, the $1\hbar\omega$(2fp) $J^{\pi} = 0^{+}$,

^{32}Na g.s. configuration is the less plausible as

- the observed population of several states cascading by γ decay to ^{31}Mg g.s. suggests a higher spin value for ^{32}Na,

- the strong β-1n feeding of the $3/2^+$ ^{31}Mg g.s. would be expected, and is not observed.

IV. SHELL MODEL CALCULATION AND COMPARISON WITH EXPERIMENT

Many of the novel aspects of nuclear structure found near the N=20 shell closure far from stability can be understood in a shell-model context, provided the valence space includes the sd shell and the lowest orbits of the fp shell. We shall approach the decays of ^{32}Na, ^{31}Na and ^{31}Mg using the same model, valence space and interaction already applied to other nuclei of the region [8,9,11]. Among the conclusions of these references one is of major importance here ; the fact that the transition from normal sd-shell nuclei to a region of deformation is predicted to take place at N=19. Therefore nuclei such as ^{32}Na(N=21), ^{31}Na(N=20) and ^{32}Mg(N=20) would belong to the deformation region [sometimes called also inversion region or intruder region, because the nuclear wave functions of the ground states and of the excited states at low energy are dominated by 2p-2h configurations, i.e. intruder configurations], while nuclei with N=18 would be fully normal and nuclei with N=19 transitional.

In the A=31 decays explored in this work we find these three sorts of nuclei. Besides, in the A=32 case the decay proceeds through the negative parity states of ^{32}Mg which are 1p-1h intruders. Therefore the comparisons between theory and experiment cover most possible situations.

A - The decay ^{31}Na → ^{31}Mg

In our calculation the ground state of ^{31}Na is $3/2^+$ in agreement with the experimental result. It is fully (90 %) dominated by configurations with two neutrons in the fp shell (intruders).

In order to have a good description of ^{31}Mg we have to enlarge slightly the valence space used in earlier calculations. The new configurations taken now into account are those with one neutron hole in the 2s1/2 shell. The reason for that is simple ; the intruder configurations of ^{31}Mg can be viewed as ^{29}Mg $\otimes$ (fp)^2 ; and, it happens that ^{29}Mg has its ground state $3/2^+$ almost degenerate with a $1/2^+$ state dominated by this kind of configuration. We are forced to include them explicitly. This is a very peculiar situation which holds only for this nucleus. Moreover, the modification of the valence space has no appreciable consequences for nuclei other than ^{31}Mg.

The resulting level scheme is plotted in Fig. 13. The correspondence with the experimental scheme is very good. From our calculation, the ground state doublet would be $3/2^+$, $1/2^+$, and the next excited state $3/2^-$. The $7/2^-$ that the calculation places degenerate with the $3/2^-$ would correspond to the experimental state at 465 keV while the second $3/2^+$ predicted at 450 keV fits with the state experimentally seen at 673 keV (see Fig.13 for a blow up of this part of the level scheme).

As it can be gathered from the comparison of the experimental and theoretical level schemes of Fig.13, many other levels are well accounted by the computation. The main failure of an sd-shell calculation, i.e. the very low density of states in the first 2 MeV of the spectrum is completely cured by our treatement. It is worth to notice here that in the best sd calculation available [32], the first excited state of ^{31}Mg lies at 1.55 MeV while our experiment places seven excited levels below this energy.

The ^{31}Mg ground state comes out as a 50 % mixing of normal and intruder components. The calculated Q_β of the decay ^{31}Na $\rightarrow$ ^{31}Mg is 15.2 MeV compared to $Q_\beta(\text{exp}) = 15.4 \pm 0.5$ MeV.

We have computed the Gamow-Teller transition probabilities for the decay of the ^{31}Na ground state to states of ^{31}Mg, with the following results :

- the half-life of ^{31}Na, computed using the bare Gamow-Teller operator is 4 ms. With the usual renormalization, which amounts to taking $(g_A/g_V)_{\text{eff}} = 0.77(g_A/g_V)_{\text{bare}}$, the half-life is 7 ms, while the experimental value is 17 ms. This discrepancy may

suggest that the ^{31}Mg physical ground state is even more dominated by the intruder states than the one predicted by our calculation.

- the fractions of beta intensity to the different ^{31}Mg states are shown in Fig.13. The agreement with the experimental I_β values is fair. The states at 0, 50 and 673 keV carry experimentally 26 %, 8 % and 5 % of the total beta intensity while the corresponding theoretical numbers are respectively 29 %, 30 % and 19 %. The main discrepancy is the lack of calculated intensity near 2.2 MeV (6 %) to cope with the 20 % of beta intensity experimentally found at 2.24 MeV.

It is rather difficult to compare our result for the half-life of ^{31}Na with the one of Ref.[32]. For, a straightforward sd-shell calculation should produce a $5/2^+$ as ground state of ^{31}Na. The authors of Ref.[32] have computed the ^{31}Na decay taking the $3/2^+$ excited state as if it were the ground state. However, the physical $3/2^+$ ground state of ^{31}Na is completely different from the sd shell $3/2^+$. Therefore, a calculation of the ^{31}Na decay based upon the sd $3/2^+$ state is not meaningful. If one plainly computes the decay of the sd ground state of ^{31}Na, i.e. $J^\pi = 5/2^+$, the predicted half-life would be 2 ms instead of the 7 ms obtained in Ref.[32] for the decay of the $3/2^+$. These arguments hold not only for the half-life calculation but also for the Gamow-Teller strength function.

The experimental values of B(GT) extracted from our measurements of the ^{31}Na decay, for the levels below 4 MeV of ^{31}Mg, are plotted in Fig.14 by summing the strength in 200 keV bins. In the same figure, are presented for comparison the predicted distributions of GT strength obtained with the sd + fp configurations. We should note that between 2.4 and 4 MeV excitation energy in ^{31}Mg, some experimental strength is missing as the delayed neutron contribution has not been taken into account in this plot.

For the states populated below 2 MeV the predicted strength exceeds the experimental value as shown in Fig.14. This result is in agreement with the general quenching factor of experiment relative to theory which has been observed in most GT decays of sd or fp nuclei.

We have also computed the electromagnetic transitions involving the three lowest levels in ^{31}Mg. The results are the following :

- The reduced transition probability $1/2^+ \rightarrow 3/2^+$ is $B(M1) = 0.98\ 10^{-2}\ \mu_N^2$. Using the experimental value $E_\gamma = 50$ keV this gives $\tau = 24$ ns in agreement with our experimental result, $\tau = 23 \pm 4$ ns.

- The reduced transition probability for the deexcitations of the $3/2^-$ to the $1/2^+$ and $3/2^+$ states are :

$$B(E1)[3/2^- \rightarrow 1/2^+] = 0.34\ 10^{-2}\ e^2\ fm^2$$
$$B(E1)[3/2^- \rightarrow 3/2^+] = 0.84\ 10^{-3}\ e^2\ fm^2$$

using the experimental values for the transitions energies E_γ we find a branching ratio 66/33 compared to the experimental result 71/29.

B - The decay ^{31}Mg $\rightarrow$ ^{31}Al

The nucleus ^{31}Al is a normal sd-shell nucleus. We have described it by means of a full sd-shell calculation using the USD (unified sd) interaction of Wildenthal [33]. To the sd states we have added the intruder states without mixing. The results are the following :

- The Q_β of the decay is in our calculation 10.6 MeV compared to the experimental result $Q_\beta = 11.69 \pm 0.27$ MeV. We shall use the experimental value in the calculation of the decay properties.

- The predicted half-life is 120 ms using the bare Gamow-Teller operator. With the renormalized operator the result is $T_{1/2} = 200$ ms compared to the experimental result $T_{1/2}(exp) = 250$ ms. The sd calculation of Ref.[32] gives a half-life of 27 ms using the renormalized operator.

- The calculated beta intensities are included in Fig.15 and the Gamow-Teller strengths shown in Fig.16. Our calculation – and also the sd calculation of Ref.[32] – put too much intensity in the ground state. Nevertheless the B(GT) representation (Fig.16) shows a general agreement between the experiment and the calculations for the location of strengths and for the first three states the intensity is better reproduced by the inclusion of the intruder configurations.

In conclusion, for A=31 our theoretical approach improves drastically the description of the level scheme of ^{31}Mg. It also explains to a large extent the existing discrepancies in the half-lifes of ^{31}Na and ^{31}Mg. The good agreement found makes it possible to establish N=19 as the place where the transition from normal to intruder dominated ground states happens in Na, Mg and Ne isotopes.

C - The decay ^{32}Na → ^{32}Mg

In this decay parent and daughter nuclei are well inside the intruder region. The results of our calculations are as follows :

- The Q_β value is found theoretically to be 18.5 MeV, as compared to Q_β(exp) = 17.4 ± 0.8 MeV.

- The spins $J^\pi = 3^-$ and 4^- for the ground state of ^{32}Na are compatible with our calculations which locates them respectively at 0 and 0.08 MeV. Therefore we have studied the ^{32}Na decay for both J^π values of the ground state.

- The calculated level scheme of ^{32}Mg has the following features ; the first excited state is a 2^+, predicted at an excitation energy of 0.81 MeV in full agreement with the experimental result (885 keV). Many other positive parity states are predicted, starting at 1.7 MeV excitation energy. These states have not been observed yet.

- The states fed in the decay of ^{32}Na are negative parity states of ^{32}Mg. Experimentally these states appear above 2.1 MeV. We have calculated them allowing 1p-1h and 3p-3h configurations to mix. Theoretically these states come out starting at 2.9 MeV excitation energy.

We have computed the transition probabilities for the Gamow-Teller decays to the available states in two cases, depending on the value $J^\pi = 3^-$ or 4^- for the ^{32}Na parent state.

In the first case, $J^\pi = 3^-$, the computed half-life is 5.4 ms using the bare Gamow-Teller operator and the experimental Q_β value and becomes 9.1 ms with the standard 0.77 renormalization. This result compares fairly well with the experimental half-life of 14.0 ms. The Gamow-Teller strength goes mainly to states around 3 MeV, with the intensity distribution reported in the left part of Table 12.

In the second case, $J^{\pi} = 4^{-}$, the half-life with the bare Gamow-Teller operator is 4.9 ms, and with the renormalized operator 8.3 ms. So no clear choice for J^{π} (^{32}Na) can be made on this basis. The Gamow-Teller strength has the structure given by the intensity distribution reported in the right part of Table 12 which is quite similar to the structure obtained in the preceeding case. If we compare with the experimental results (Table 10) we see that both calculations have the same -and very frequent- defect of predicting too much beta intensity in the few lowest states.

D - Concluding remarks

The new experimental results presented in this work can be adequately accounted for in a model of the region N=20 far from the stability which includes in the valence space the intruder configurations obtained by promoting two sd shell neutrons to the fp shell. To the previous experimental results establishing the existence of a region of intruder dominance at N=20, namely the well known spin anomaly of ^{31}Na and the extremely low 2^{+} state of ^{32}Mg, one adds now the low energy level scheme and the Gamow-Teller distribution of ^{31}Mg to define N=19 as the neutron number at which the transition takes place.

REFERENCES

[1] C. Thibault, R. Klapisch, C. Rigaud, A.M. Poskanzer, R. Prieels, L. Lessard and W. Reisdorf, Phys. Rev. C12, 644 (1975)

[2] C. Detraz, M. Langevin, M.C. Goffri-Kouassi, D. Guillemaud, M. Epherre, G. Audi, C. Thibault and F. Touchard, Nucl. Phys. A394, 378 (1983)

[3] C. Detraz, D. Guillemaud, G. Huber, R. Klapisch, M. Langevin, F. Naulin, C. Thibault, L.C. Carraz and F. Touchard, Phys. Rev. C19, 164 (1979)

[4] B.H. Wildenthal and W. Chung, Phys. Rev. C22, 2260 (1980)

[5] P.M. Endt, Nucl. Phys. A521, 364 (1990)

[6] X. Campi, H. Flocard, A.K. Kerman and S. Koonin, Nucl. Phys. A251, 193 (1975)

[7] A. Watt, R.P. Singhal, M.H. Storm and R.R. Whitehead, J. Phys. G7, L145 (1981)

[8] A. Poves and J. Retamosa, Phys. Lett. B184, 311 (1987)

A. Poves, Proc. Workshop Nuclear Structure of Light Nuclei Far From Stability, Obernai (1989), edited by G. Klotz, CRN Strasbourg, p.101

[9] P. Baumann, A. Huck, G. Klotz, A. Knipper, G. Walter, G. Marguier, H.L. Ravn, C. Richard-Serre, A. Poves and J. Retamosa, Phys. Lett. B228, 458 (1989)

[10] E.K. Warburton, J.A. Becker and B.A. Brown, Phys. Rev. C41, 1147 (1990)

B.A. Brown, E.K. Warburton and B.H. Wildenthal, Proc. Workshop Nuclear Structure of Light Nuclei Far From Stability, Obernai (1989), edited by G. Klotz, CRN Strasbourg, p.147

[11] A. Poves and J. Retamosa, to be published

[12] N. Fukunishi and T. Otsuka (1991)

[13] K. Heyde, Proc. Workshop Nuclear Structure of Light Nuclei Far From Stability, Obernai (1989), edited by G. Klotz, CRN Strasbourg, p.129

K. Heyde and J.L. Wood, J. Phys. G : Nucl. Part. Phys. 17, 135 (1991)

[14] K. Heyde, P. Van Isacker, M. Waroquier, J.L. Wood and R.A. Meyer, Phys. Repts. 102, 291 (1983)

[15] S.K. Patra and C.R. Praharaj, Phys. Lett. B273, 13 (1991)

[16] A. Gillibert, W. Mittig, L. Bianchi, A. Cunsolo, B. Fernandez, A. Foti, J. Gastebois, C. Gregoire, Y. Schutz and C. Stephan, Phys. Lett. B192, 39 (1987)

[17] D.J. Vieira, J.M. Wouters, K. Vaziri, J.R.H. Kraus, H. Wollnik, G.W. Butler, F.K. Wohn and A.H. Wapstra, Phys. Rev. Lett. 57, 3253 (1986)

[18] N.A. Orr, W. Mittig, L.K. Fifield, M. Lewitowicz, E. Plagnol, Y. Schutz, Zhan Wen Long, L. Bianchi, A. Gillibert, A.V. Belozyorov, S.M. Lukyanov, Yu.E. Penionzhkevich, A.C.C. Villari, A. Cunsolo, A. Foti, G. Audi, C. Stephan and L. Tassan-Got, Phys. Lett. B258, 29 (1991)

[19] X.G. Zhou, X.L. Tu, J.M. Wouters, D.J. Vieira, K.E.G. Löbner, H.L. Seifert, Z.Y. Zhou and G.W. Butler, Phys. Lett. B260, 285 (1991)

[20] D. Guillemaud-Mueller, C. Detraz, M. Langevin, F. Naulin, M. de Saint-Simon, C. Thibault, F. Touchard and M. Epherre, Nucl. Phys. A426, 37 (1984)

[21] C.L. Woods, W.N. Catford, L.K. Fifield, N.A. Orr and R.J. Sadleir, Nucl. Phys. A476, 392 (1988)

[22] L.K. Fifield, C.L. Woods, R.A. Bark, P.V. Drumm and M.A.C. Hotchkis, Nucl. Phys. A440, 531 (1985)

[23] L.K. Fifield, C.L. Woods, W.N. Catford, R.A. Bark, P.V. Drumm and K.T. Keoghan, Nucl. Phys. A453, 497 (1986)

[24] G. Walter, P. Baumann, A. Huck, G. Klotz, A. Knipper, G. Marguier, H.L. Ravn, C. Richard-Serre, A. Poves and J. Retamosa, Proc. Workshop Nuclear Structure of Light Nuclei Far From Stability, Obernai (1989), edited by G. Klotz, CRN Strasbourg, p.85

[25] A. Huck, G. Klotz, A. Knipper, Ch. Miehé, C. Richard-Serre, G. Walter, A. Poves, H.L. Ravn and G. Marguier, Phys. Rev. C31, 2226 (1985)

[26] A.H. Wapstra and G. Audi, Nucl. Phys. A432, 1 (1985)
A.H. Wapstra, G. Audi and R. Hoekstra, At. Data and Nucl. Data Tables 39, 281 (1988)

[27] G. Huber, F. Touchard, S. Bütgenbach, C. Thibault, R. Klapisch, H.T. Duong, S. Liberman, J. Pinard, J.L. Vialle, P. Juncar and P. Jacquinot, Phys. Rev. C18, 2342 (1978)

[28] M. Langevin, C. Detraz, D. Guillemaud-Mueller, C. Thibault, F. Touchard and M. Epherre, Nucl. Phys. A414, 151 (1984)

[29] G. Walter, P. Baumann, M. Bounajma, Ph. Dessagne, A. Huck, G. Klotz, A. Knipper, Ch. Miehé, J. Rachidi, M. Ramdane, G. Marguier, C. Richard-Serre, A. Dobado and A. Poves, Proc. Workshop Nuclear Structure of Light Nuclei Far From Stability, Obernai (1989), edited by G. Klotz, CRN Strasbourg, p.71

[30] P. Baumann, Ph. Dessagne, A. Huck, G. Klotz, A. Knipper, G. Marguier, Ch. Miehé, M. Ramdane, C. Richard-Serre, G. Walter and B.H. Wildenthal, Phys. Rev. C36, 765 (1987)

[31] P. Baumann, Ph. Dessagne, A. Huck, G. Klotz, A. Knipper, Ch. Miehé, M. Ramdane, G. Walter, G. Marguier, H. Gabelmann, C. Richard-Serre, K. Schlösser and A. Poves, Phys. Rev. C39, 626 (1989)

[32] B.H. Wildenthal, M.S. Curtin and B.A. Brown, Phys. Rev. C28, 1343 (1983)

[33] B.H. Wildenthal, Prog. Part. Nucl. Phys. 11, 5 (1983)

TABLE CAPTIONS

Table I Energy and intensity of γ rays observed in the β decay of ^{31}Na.

Table II Gamma ray branching ratios in ^{31}Mg.

Table III Beta intensities and log ft values in the ^{31}Na β decay to bound levels in ^{31}Mg.

Table IV Energy and intensity of γ rays observed in the β decay of ^{31}Na and related to the β-delayed 1n-channel.

Table V Intensity of neutron branches populating excited states in ^{30}Mg.

Table VI Energy and intensity of γ rays observed in the β decay of ^{31}Mg.

Table VII Gamma ray branching ratios in ^{31}Al.

Table VIII Beta intensities and log ft values in the ^{31}Mg β decay to bound levels in ^{31}Al.

Table IX Energy and intensity of γ rays observed in the β decay of ^{32}Na.

Table X Beta branch intensities and corresponding log ft values in the partial decay scheme of ^{32}Na to ^{32}Mg levels.

Table XI Neutron branching ratios in the one- and two-neutron β-delayed channels of the ^{32}Na decay scheme.

Table XII Calculated β intensities in the decay of ^{32}Na : left part corresponds to $J^{\pi} = 3^-$ for ^{32}Na ground state, right part to $J^{\pi} = 4^-$.

TABLE I

E_γ[a] (keV)	I_γ (relative)	I_γ (per 100 decays)	Transition[a] (MeV)
50.5 ± 0.7	125.4 ± 15.5	19.5 ± 3.9	0.050 - 0
54.6 ± 0.1[b]			0.055 - 0[d]
170.5 ± 0.5	35.0 ± 2.0	5.4 ± 0.9	0.22 - 0.050
221.0 ± 0.5	14.2 ± 1.1	2.2 ± 0.4	0.22 - 0.050
305.6 ± 0.3[c]	13.6 ± 1.3	2.0 ± 0.7	1.79 - 1.48[c]
451.1 ± 1.1	2.9 ± 0.8	0.4 ± 0.1	0.67 - 0.22
622.6 ± 1.4	23.0 ± 1.8	3.6 ± 0.6	0.67 - 0.050
673.1 ± 1.2	11.6 ± 0.9	1.8 ± 0.3	0.67 - 0
807.6 ± 0.6	9.4 ± 1.4	1.5 ± 0.3	1.03 - 0.22
894.6 ± 0.7	5.8 ± 1.2	0.9 ± 0.2	0.94 - 0.050
985.1 ± 0.4[c]	12.0 ± 2.2[e]	1.8 ± 0.7	2.47 - 1.48[c]
1039.9 ± 0.2[d]	0.20 ± 0.06	0.03 ± 0.01	1.09 - 0.055[d]
1214.7 ± 0.9	10.0 ± 1.0	1.6 ± 0.3	2.24 - 1.03
1482.0 ± 0.3[c]	100	15.0 ± 5.0	1.48 - 0[c]
1571.1 ± 1.2	16.8 ± 1.9	2.6 ± 0.5	3.81 - 2.24
1638.0 ± 0.2[d]	0.10 ± 0.04	0.02 ± 0.01	1.64 - 0[d]
1820.2 ± 0.6[c]	20.0 ± 2.2[d]	3.0 ± 1.0	1.82 - 0[c]
1978.0 ± 0.6[c]	29.2 ± 2.6	4.4 ± 1.5	3.46 - 1.48[c]
2022.0 ± 0.7	28.9 ± 3.1	4.5 ± 0.9	2.24 - 0.22
2192.8 ± 0.6	25.6 ± 2.6	4.0 ± 0.8	2.24 - 0.050
2243.5 ± 0.6	86.0 ± 5.0	13.3 ± 2.3	2.24 - 0
3537.7 ± 1.2	7.8 ± 1.6	1.2 ± 0.3	3.76 - 0.22
3710.0 ± 2.0	4.0 ± 2.3	0.6 ± 0.4	3.76 - 0.050
3761.1 ± 2.0	5.7 ± 2.1	0.9 ± 0.4	3.76 - 0

[a] In ^{31}Mg unless otherwise specified.

[b] Present in the decay scheme of ^{29}Na (Ref. [30]), produced here in the 2n-channel but its intensity could not be reliably appraised because of the close neighbourhood of the strong 50.5 keV line.

[c] In ^{30}Mg : subsequent to β-delayed one-neutron emission.

[d] In ^{29}Mg : subsequent to β-delayed two-neutron emission offering an observable strength.

[e] Adopted value from Ref. [20] because of the presence in our spectrum of a contaminating line at this energy.

TABLE II

E_i (keV)	E_f (keV)	Gamma branching ratio
50	0	100
221	0	29 ± 2
	50	71 ± 2
673	0	28 ± 2
	50	64 ± 3
	221	8 ± 2
945	50	100
1029	221	100
2243	0	58 ± 2
	50	17 ± 2
	221	19 ± 2
	1029	6 ± 1
3760	0	33 ± 10
	50	23 ± 11
	221	44 ± 10
3814	2243	100

TABLE III

E_x (keV)	$I\beta$ (per 100 decays)	log ft
0	26 ± 9	4.9
50.5 ± 0.7	4.8 ± 3.2	5.6
221.0 ± 0.4	< 2.2	> 6.0
673.1 ± 1.2	5.3 ± 1.6	5.5
945.1 ± 1.0	0.9 ± 0.3	6.2
1028.6 ± 0.8	< 1.1	> 6.1
2243.5 ± 0.4	19.7 ± 5.9	4.7
2759.9 ± 1.0	2.6 ± 0.9	5.3
3814.5 ± 1.3	2.5 ± 0.8	5.3

TABLE IV

E_γ (keV)	I_γ (relative)	I_γ (per 100 decays)
305.6 ± 0.3	13.6 ± 1.3	2.0 ± 0.7
985.1 ± 0.4	12.0 ± 2.2[a]	1.8 ± 0.7
1482.0 ± 0.3	100	15.0 ± 5.0
1820.2 ± 0.6	20.0 ± 2.2[a]	3.0 ± 1.0
1978.0 ± 0.6	29.2 ± 2.6	4.4 ± 1.5

[a] values taken from Ref. [20] because of a contamination in our spectrum.

TABLE V

$E_x(^{30}Mg)$ (keV)	I_n (per 100 decays)
0	19.3 ± 5.7[a]
1482	6.8 ± 1.4
1788	2.0 ± 0.3
1820	3.0 ± 0.5
2467	1.8 ± 0.4
3460	4.4 ± 0.7

[a] deduced from the P_n value (37.3±5.4 %) and from the absolute neutron branch intensity to excited levels (18.0± 1.7 %).

TABLE VI

E_γ (keV)	I_γ (relative)	I_γ (per 100 decays)	Transition (MeV)
666.2 ± 0.7	34.0 ± 1.8	13.4 ± 2.3	1.61 - 0.95
904.0 ± 0.8	5.3 ± 0.6	2.1 ± 0.4	4.14 - 3.24
946.6 ± 0.5	78.3 ± 4.0	30.8 ± 5.2	0.95 - 0
1612.8 ± 0.4	100(±5.1)	39.4 ± 6.6	1.61 - 0
1626.2 ± 0.5	63.6 ± 3.3	25.1 ± 4.2	3.24 - 1.61
1820.0 ± 0.8	8.8 ± 1.2	3.5 ± 0.7	3.43 - 1.61
2487.6 ± 1.5	4.8 ± 0.8	1.9 ± 0.4	3.43 - 0.95
2529.8 ± 1.0	8.7 ± 0.8	3.4 ± 0.6	4.14 - 1.61
2676.1 ± 1.0	7.7 ± 0.8	3.0 ± 0.6	3.62 - 0.95
2949.0 ± 1.0	12.3 ± 1.1	4.8 ± 0.9	4.56 - 1.61
3196.2 ± 1.0	13.0 ± 1.3	5.1 ± 1.0	4.14 - 0.95
3431.8 ± 1.2	16.2 ± 1.3	6.4 ± 1.1	3.43 - 0
3621.9 ± 1.3	18.2 ± 1.3	7.2 ± 1.3	3.62 - 0
4201.1 ± 1.4	5.7 ± 0.9	2.2 ± 0.5	5.15 - 0.95
4809.0 ± 1.5	2.3 ± 0.6	0.9 ± 0.3	4.81 - 0

TABLE VII

E_i (keV)	E_f (keV)	gamma branching ratio
947	0	100
1613	0	75 ± 2
	947	25 ± 2
3239	1613	100
3434	0	54 ± 1
	947	16 ± 1
	1613	30 ± 1
3622	0	70 ± 1
	947	30 ± 1
4143	947	48 ± 1
	1613	32 ± 1
	3239	20 ± 1
4562	1613	100
4809	0	100
5148	947	100

TABLE VIII

E_x (keV)	$I\beta$ (per 100 decays)	log ft
0	12.9 ± 6.0	5.8
947	5.2 ± 2.1	6.0
1613	16.1 ± 3.7	5.3
3239	23.1 ± 4.0	4.9
3434	11.7 ± 2.1	5.1
3622	10.3 ± 1.8	5.1
4143	10.7 ± 1.8	5.0
4562	4.9 ± 0.9	5.1
4809	0.9 ± 0.2	5.8
5148	2.3 ± 0.5	5.4

TABLE IX

E_γ[a] (keV)	I_γ (relative)	I_γ (per 100 decays)	Transition[a] (MeV)
50[b,c]			0.05 - 0[c]
171[c]	21.9 ± 3.5	13.3 ± 2.5	0.22 - 0.05[c]
221[c]	8.9 ± 1.8	5.4 ± 1.3	0.22 - 0[c]
240[c]	9.7 ± 1.1	5.9 ± 1.0	0.46 - 0.22[c]
694	3.8 ± 1.6[e]	2.2 ± 1.3	
885	100	58.8 ± 7.9	0.88 - 0
895[c]	5.1 ± 2.6	3.1 ± 1.6	0.94 - 0.05[c]
929[c]	4.0 ± 1.9	2.4 ± 1.2	1.39 - 0.46[c]
1232	4.8 ± 1.7	2.8 ± 1.0	2.12 - 0.88
1436	9.8 ± 2.5	5.8 ± 1.6	2.32 - 0.88
1482[d]	4.9 ± 2.2	3.0 ± 1.4	1.48 - 0[d]
1783	8.3 ± 2.0[e]	4.9 ± 1.3	4.82 - 3.04
1973	19.7 ± 2.5	11.6 ± 2.5	2.86 - 0.88
2152	48.5 ± 3.7	28.5 ± 4.1	3.04 - 0.88
2551	10.2 ± 2.5	6.0 ± 1.6	2.55 - 0
3935	18.3 ± 3.7	10.8 ± 2.6	4.82 - 0.88

[a] In ^{32}Mg unless otherwise specified.

[b] Known to occur in the ^{31}Mg deexcitation but its intensity could not be reliably determined because of the closeness of the experimental threshold.

[c] Subsequent to β-delayed one-neutron emission.

[d] Subsequent to β-delayed two-neutron emission.

[e] Adopted value from Ref. [20] because of the presence in our spectrum of a contamining line at this energy.

TABLE X

E_x (keV)	$I\beta$ (per 100 decays)	log ft
0	-	-
885	-	-
2117	2.8 ± 1.0	5.8
2321	5.8 ± 1.6	5.4
2551	6.0 ± 1.6	5.4
2858	11.6 ± 2.5	5.1
3037	23.6 ± 4.3	4.7
4820	15.7 ± 2.9	4.6

TABLE XI

One-neutron channel		Two-neutron channel	
E_x (keV)	In (per 100 decays)	E_x (keV)	I_n (per 100 decays)
0	-	0	5.3 ± 2.5[a]
50	-	1482	3.0 ± 1.4
221	12.8 ± 3.0		
461	3.5 ± 1.6		
945	3.1 ± 1.6		
1390	2.4 ± 1.2		

[a] deduced from the P_{2n} value (Ref. [28]) and the absolute γ strength emitted by ^{30}Mg.

TABLE XII

^{32}Na(g.s.) $J^{\pi} = 3^-$			^{32}Na(g.s.) $J^{\pi} = 4^-$		
$E_x(^{32}Mg)$ (MeV)	J^{π}	% β	$E_x(^{32}Mg)$ (MeV)	J^{π}	% β
2.90	3^-	9.	2.90	3^-	65.
2.91	2^-	71.			
2.95	2^-	6.			
			3.17	5^-	1.
			3.19	4^-	1.
3.29	3^-	4.	3.29	3^-	2.
3.60	3^-	2.	3.60	3^-	9.
			3.62	4^-	2.
3.73	2^-	3.			
			3.96	5^-	4.
			4.02	4^-	1.
			4.41	4^-	2.
4.48	2^-	1.			
			4.79	4^-	1.
5.64	4^-	1.	5.64	4^-	2.

FIGURE CAPTIONS

Figure 1 Disintegration scheme of ^{31}Na.

Figure 2 Delayed coincidences taken in the decay of ^{31}Na with the NE102 plastic β detector and a small BaF_2 scintillator. In the inset the decay curve of the 50 keV gate, a least squares fit leads to the value of $T_{1/2}$ = 16.0 ± 2.8 ns.

Figure 3 Partial view of the 50 keV ray gated spectrum showing the substantial enhancement of the 623 keV line superposed on the longer-lived component due to the descendant, the prominent 171 keV peak, a weak line at 452 keV and two rays at 808 and 895 keV. The lower part of the figure is the corresponding background.

Figure 4 Partial view of the 171 keV gate showing the presence of the 452 keV line along with the 808 keV one. In the lower part corresponding to the background, the contaminating lines are labelled by the parent isotope.

Figure 5 A partial γ spectrum of the ^{31}Na (β^-,γ) decay is shown in the top part of the figure and compared in the same energy range to the spectrum taken in coincidence with neutrons, in bottom part. Note the enhancement of the γ lines subsequent to the 1n-process ; lines arising in the 2n-process (e.g. 1041 keV) are not substantially favoured by the coincidence technique, probably because of the energy threshold in the neutron detection chain.

Figure 6 Disintegration scheme of ^{31}Mg. The column at the right gives the theoretical J^{π} values from Ref. [32].

Figure 7 Gate on the 947 keV line corresponding to the deexcitation of the first level in ^{31}Al. The lower part of the figure shows the corresponding background. These results support the whole framework of the proposed ^{31}Mg decay scheme.

Figure 8 Upper left : gate on the 1626 keV line emphasizing the components of the 4143 → 3239 → 1613 → 947 → 0 cascade (background below).
Upper right : gate on the 3196 keV line showing the outstanding presence of the 947 keV transition whereas the 666 keV peak does not exhibit the expected strength if the 3196 keV ray assignment of Ref. [20] is assumed. However, a weak contribution of this process cannot be excluded.

Figure 9 Decay scheme for ^{32}Na → ^{32}Mg and the competing neutron emission.

Figure 10 Upper left and bottom left : gates on the 1436 and 1232 keV lines revealing the population of the first excited state of ^{32}Mg (background has been subtracted). The right part shows the evidence for a cascade in the ^{32}Mg → ^{32}Al decay.

Figure 11 Comparison of the direct γ spectrum of the ^{32}Na (β^-,γ) process to the γ spectrum taken in coincidence with neutrons. The enhancement of the lines at 171, 221, 240 and 929 keV (not shown) provides a clear evidence for the population of a set of levels in ^{31}Mg distinct from those populated in the ^{31}Na decay.

Figure 12 The gate on the 240 keV peak, in the γ-γ coincidences, from the ^{32}Na decay, establishes the cascade relations of the set of levels revealed by the n,γ coincidences (background in the lower part of the figure).

Figure 13 Comparison of experimental and theoretical level stucture of ^{31}Mg and β intensities from the ^{31}Na decay. On the right blow up of the first excited states.

Figure 14 Comparison of experimental (top part of the figure) and theoretical B(GT) distributions in the ^{31}Na → ^{31}Mg decay plotted by summing the strengths within each 200 keV energy interval.

Figure 15 Comparison of experimental and theoretical level structure of ^{31}Al and β intensities from the ^{31}Mg decay.

Figure 16 Comparison of theoretical and experimental B(GT) distributions in the ^{31}Mg → ^{31}Al decay : the upper part shows the experimental data, the middle part, calculations from Ref. [32] and the lower part calculations corresponding to this work.

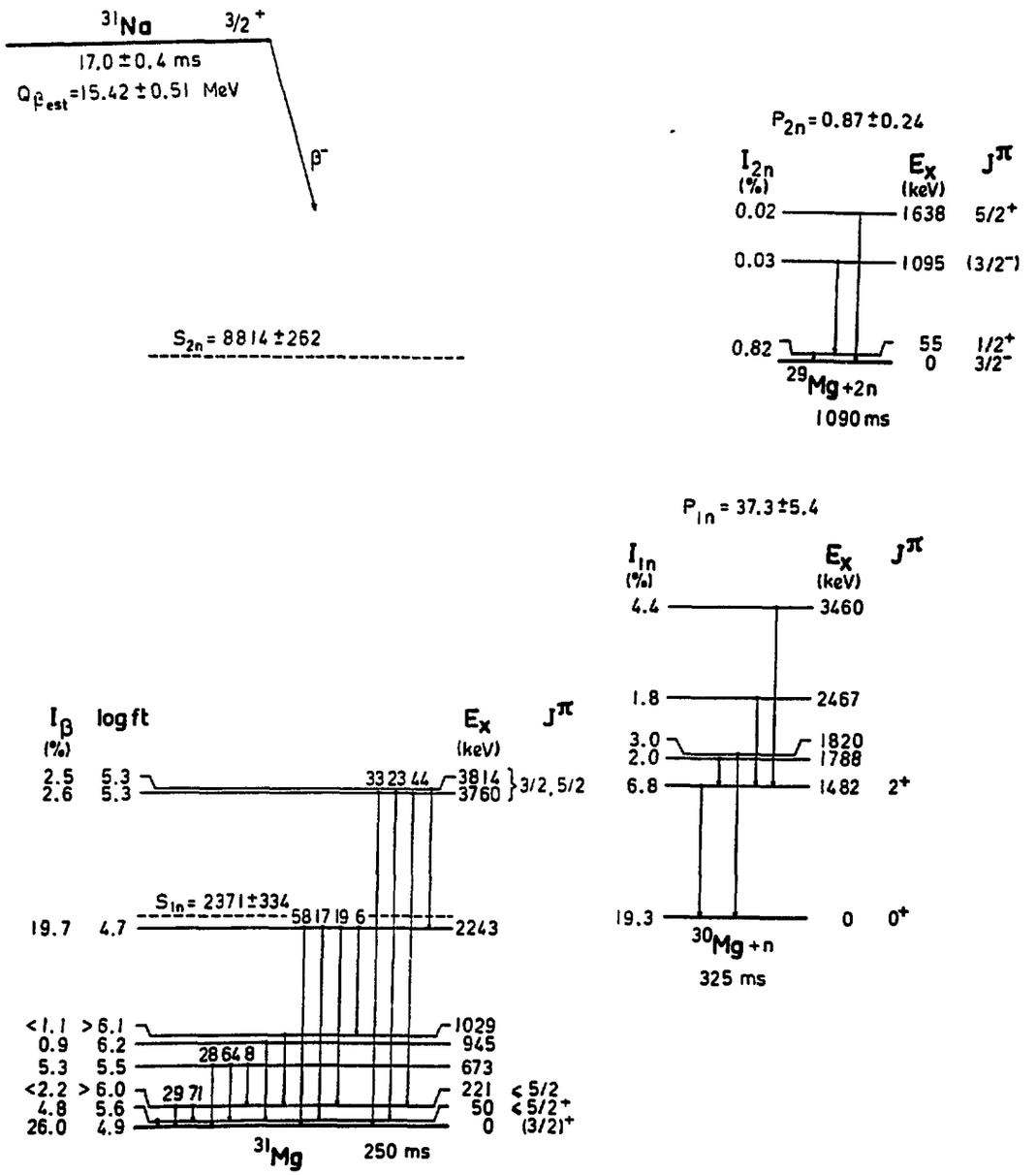
31Na 3/2+
17.0 ± 0.4 ms
Qβ est = 15.42 ± 0.51 MeV
β-
S2n = 8814 ± 262
P2n = 0.87 ± 0.24
I2n (%)
Ex (keV)
Jπ
0.02 1638 5/2+
0.03 1095 (3/2-)
0.82 55 1/2+
0 3/2-
29Mg + 2n
1090 ms
P1n = 37.3 ± 5.4
I1n (%)
Ex (keV)
Jπ
4.4 3460
1.8 2467
3.0 1820
2.0 1788
6.8 1482 2+
19.3 0 0+
30Mg + n
325 ms
Iβ (%)
log ft
Ex (keV)
Jπ
2.5 5.3 3814
2.6 5.3 3760
3.3 2.3 4.4
3/2, 5/2
S1n = 2371 ± 334
5.8 1.7 1.9 6
19.7 4.7 2243
<1.1 >6.1 1029
0.9 6.2 945
2.8 6.4 8
5.3 5.5 673
<2.2 >6.0 2.9 7.1 221 ≤ 5/2
4.8 5.6 50 ≤ 5/2+
26.0 4.9 0 (3/2)+
31Mg
250 ms

Fig.1

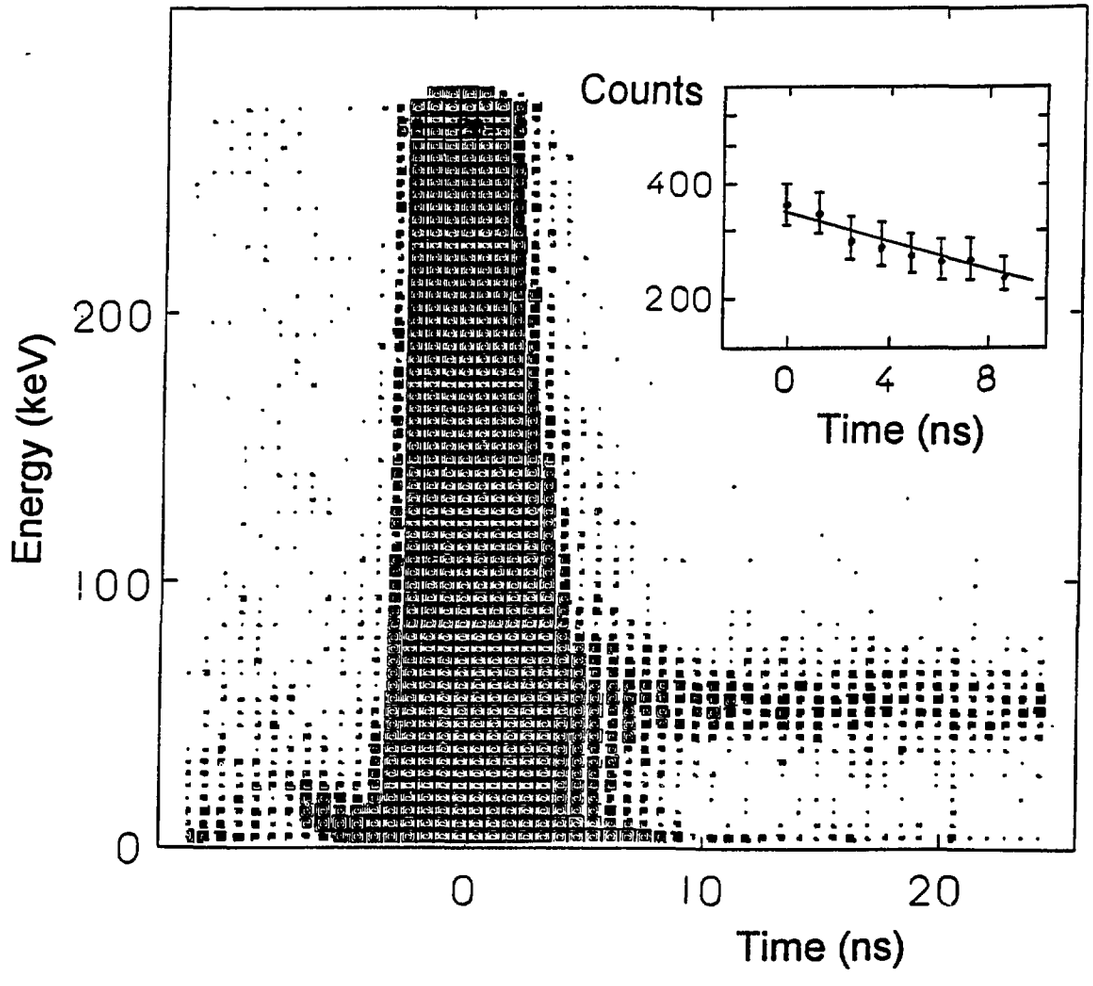

Fig.2

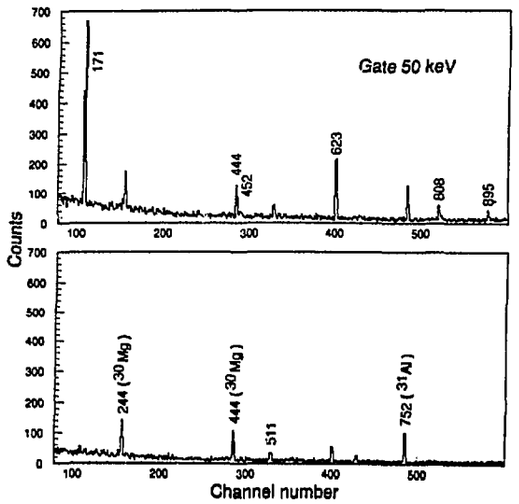
Gate 50 keV
171
444
452
623
808
895
244 (30Mg)
444 (30Mg)
511
752 (31Al)
Counts
Channel number

Fig.3

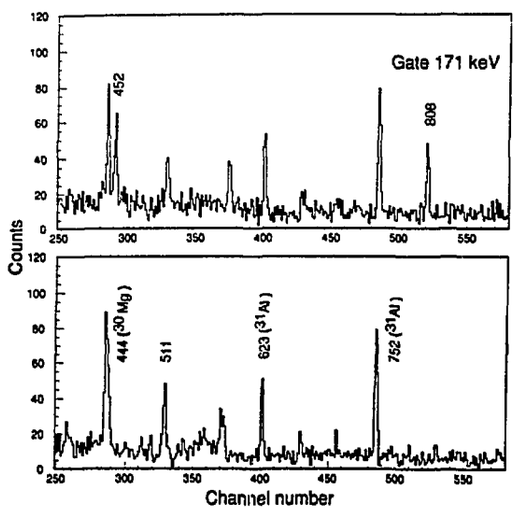
Gate 171 keV
452
808
444 (30Mg)
511
623 (31Al)
752 (31Al)
Counts
Channel number

Fig.4

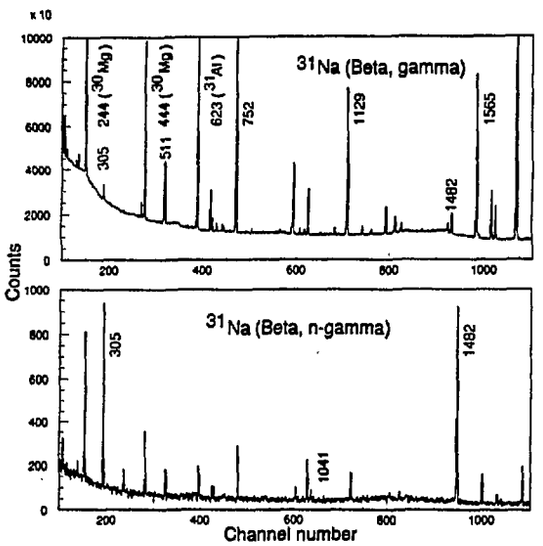
x 10
10000
8000
6000
4000
2000
0
Counts
^{31}Na (Beta, gamma)
244 (^{30}Mg)
305
444 (^{30}Mg)
511
623 (^{31}Al)
752
1129
1482
1565
200
400
600
800
1000
^{31}Na (Beta, n-gamma)
305
1041
1482
Channel number

Fig.5

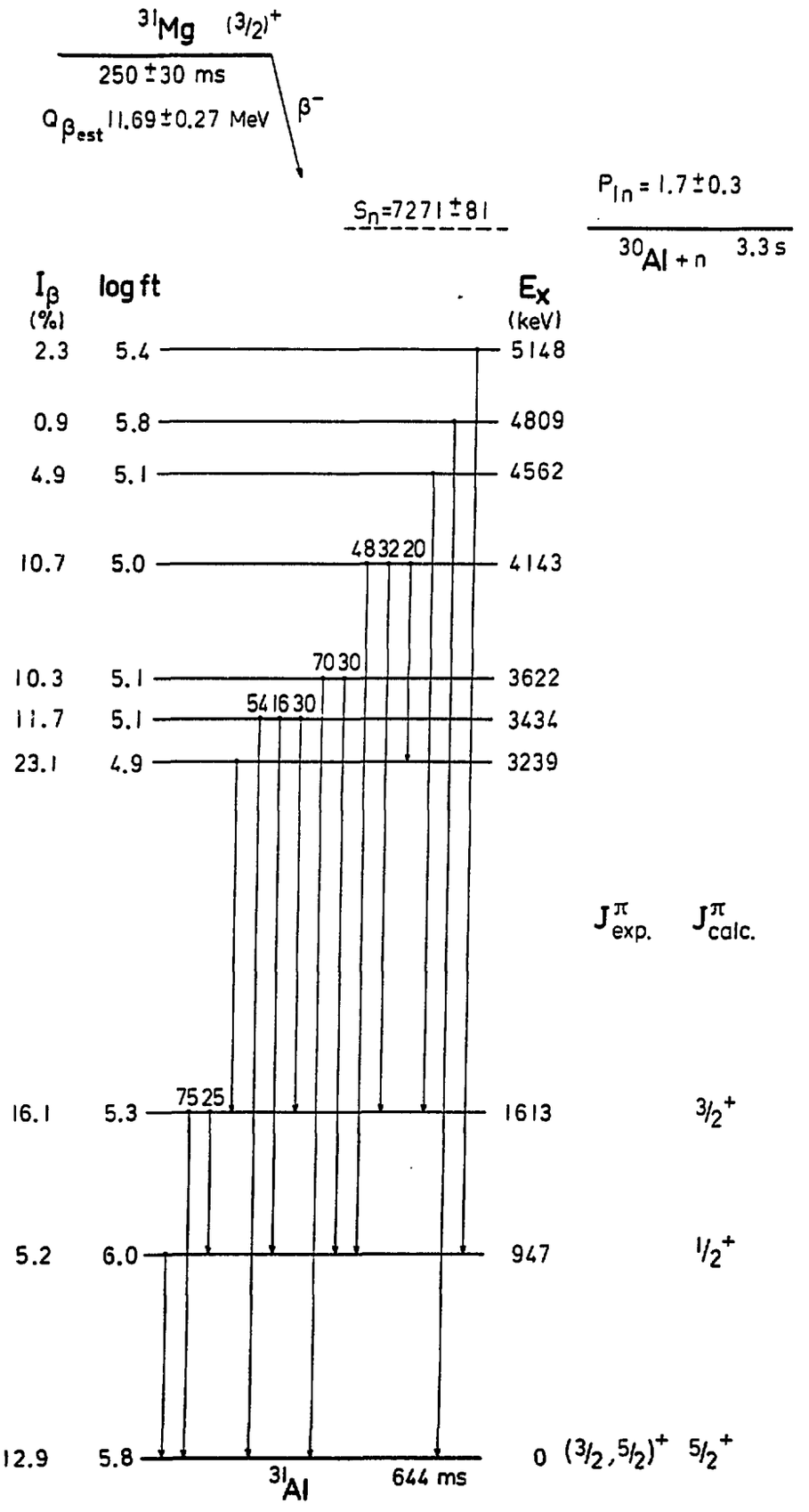
31Mg (3/2)+
250 ± 30 ms
Qβest 11.69 ± 0.27 MeV
β−
Sn=7271±81
Pln = 1.7 ± 0.3
30Al + n 3.3 s
Iβ (%)
log ft
Ex (keV)
2.3 5.4 5148
0.9 5.8 4809
4.9 5.1 4562
10.7 5.0 4143
48 32 20
10.3 5.1 3622
70 30
11.7 5.1 3434
54 16 30
23.1 4.9 3239
Jπexp. Jπcalc.
16.1 5.3 1613 3/2+
75 25
5.2 6.0 947 1/2+
12.9 5.8 0 (3/2,5/2)+ 5/2+
31Al 644 ms

Fig.6

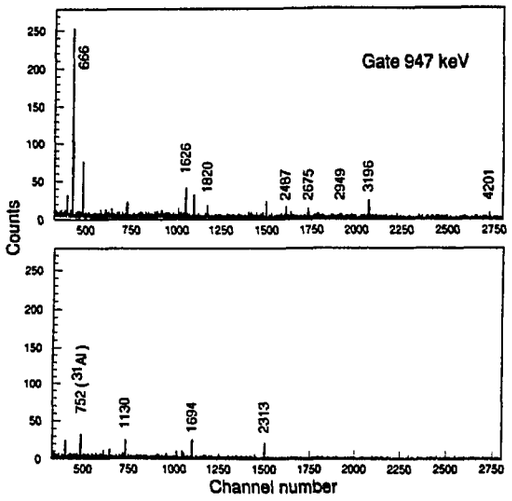
Gate 947 keV
666
1626
1820
2487
2575
2949
3196
4201
752 (31Al)
1130
1694
2313
Counts
Channel number

Fig.7

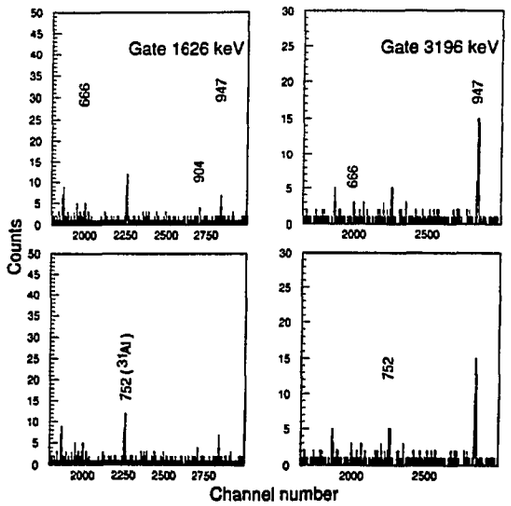
Gate 1626 keV
Gate 3196 keV
666
947
904
752 (31Al)
752
Counts
Channel number

Fig.8

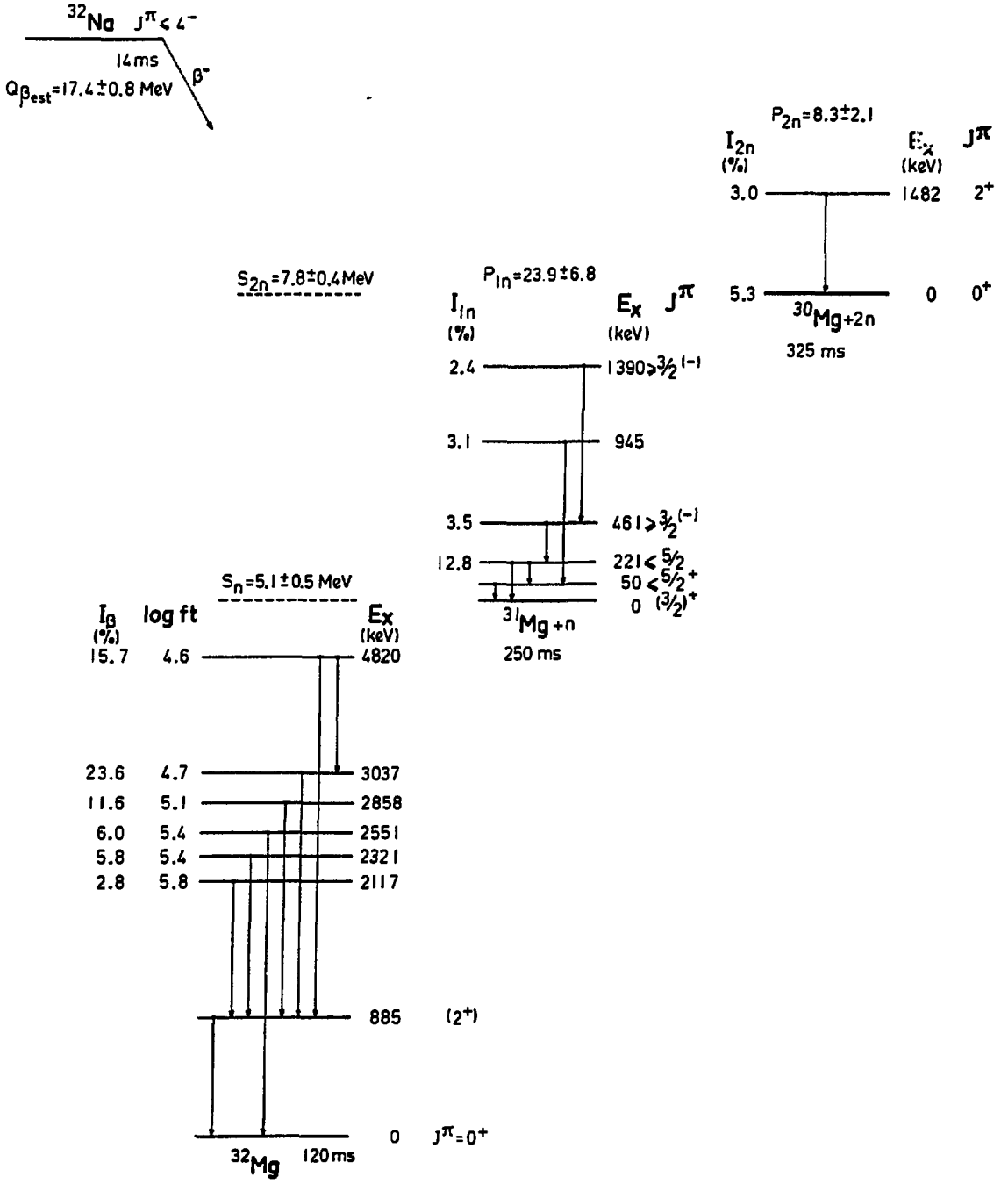
32Na Jπ< 4−
14ms
β−
Qβest=17.4±0.8 MeV
P2n=8.3±2.1
I2n (%)
Ex (keV)
Jπ
3.0
1482
2+
5.3
0
0+
30Mg+2n
325 ms
S2n=7.8±0.4MeV
P1n=23.9±6.8
I1n (%)
Ex (keV)
Jπ
2.4
1390
3/2(−)
3.1
945
3.5
461
3/2(−)
12.8
221
5/2
50
5/2+
0
(3/2)+
31Mg+n
250 ms
Sn=5.1±0.5 MeV
Iβ (%)
log ft
Ex (keV)
15.7
4.6
4820
23.6
4.7
3037
11.6
5.1
2858
6.0
5.4
2551
5.8
5.4
2321
2.8
5.8
2117
885
(2+)
0
Jπ=0+
32Mg
120ms

Fig.9

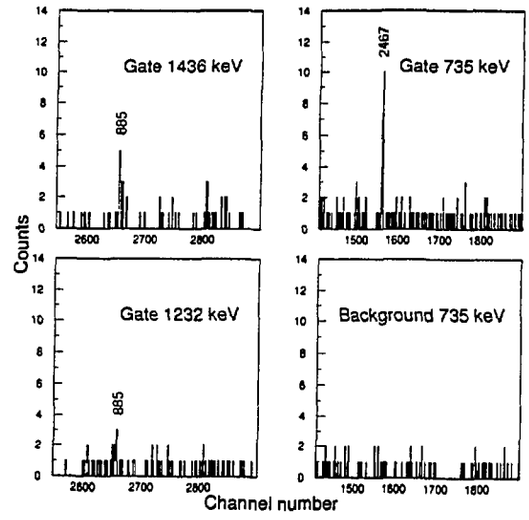
Gate 1436 keV
885
Gate 735 keV
2467
Gate 1232 keV
885
Background 735 keV
Counts
Channel number

Fig.10

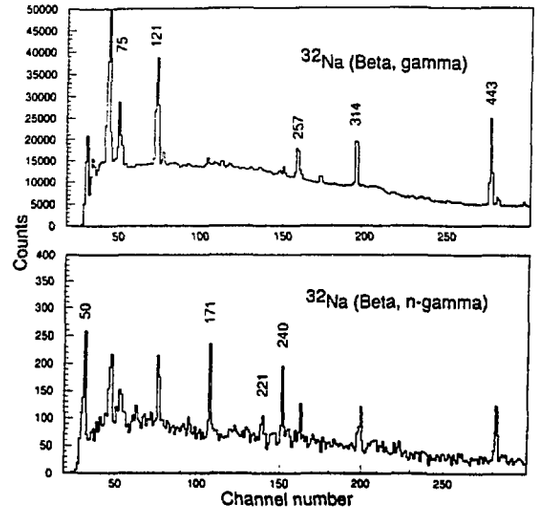
75
121
257
314
443
32Na (Beta, gamma)
50
171
240
221
32Na (Beta, n-gamma)
Counts
Channel number

Fig.11

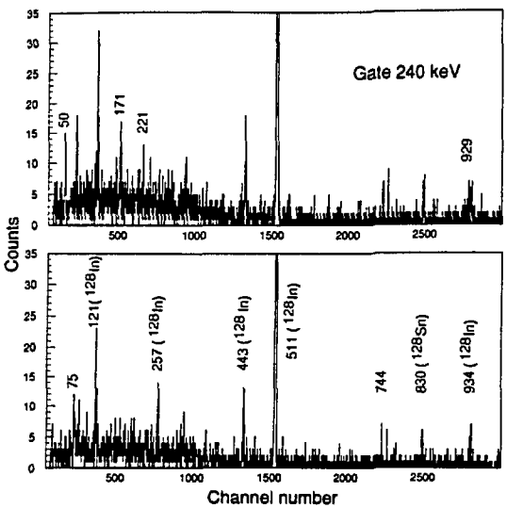
Gate 240 keV
50
171
221
929
Counts
121(128In)
75
257 (128In)
443 (128 In)
511 (128In)
744
830 (126Sn)
934 (128In)
Channel number

Fig.12

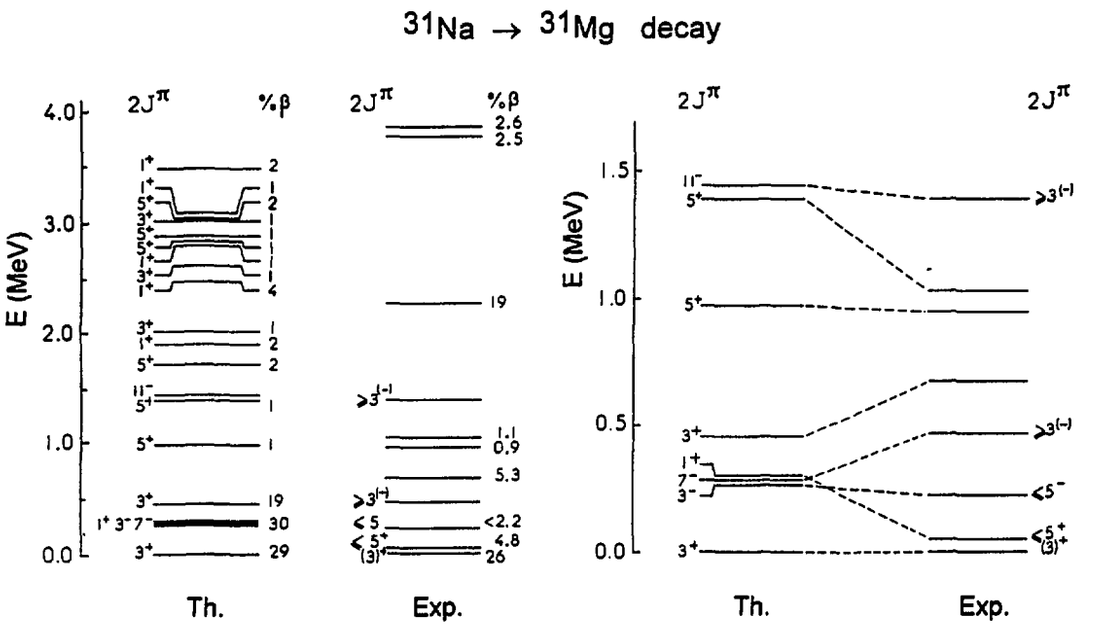

Fig. 13

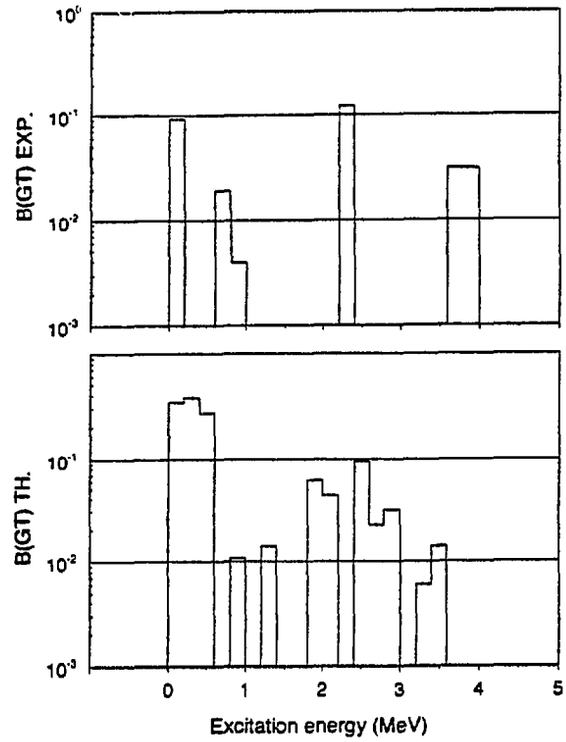

Fig.14

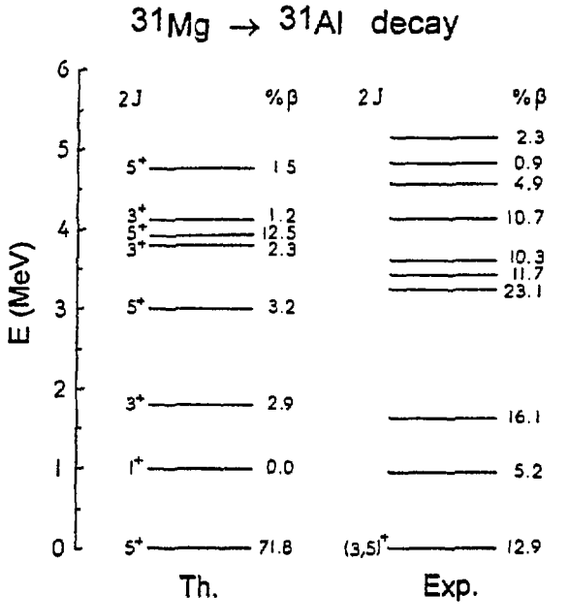
31Mg → 31Al decay
E (MeV)
2J
%β
5+ 1.5
3+ 1.2
5+ 12.5
3+ 2.3
5+ 3.2
3+ 2.9
1+ 0.0
5+ 71.8
Th.
2J
%β
2.3
0.9
4.9
10.7
10.3
11.7
23.1
16.1
5.2
(3,5)+ 12.9
Exp.

Fig.15

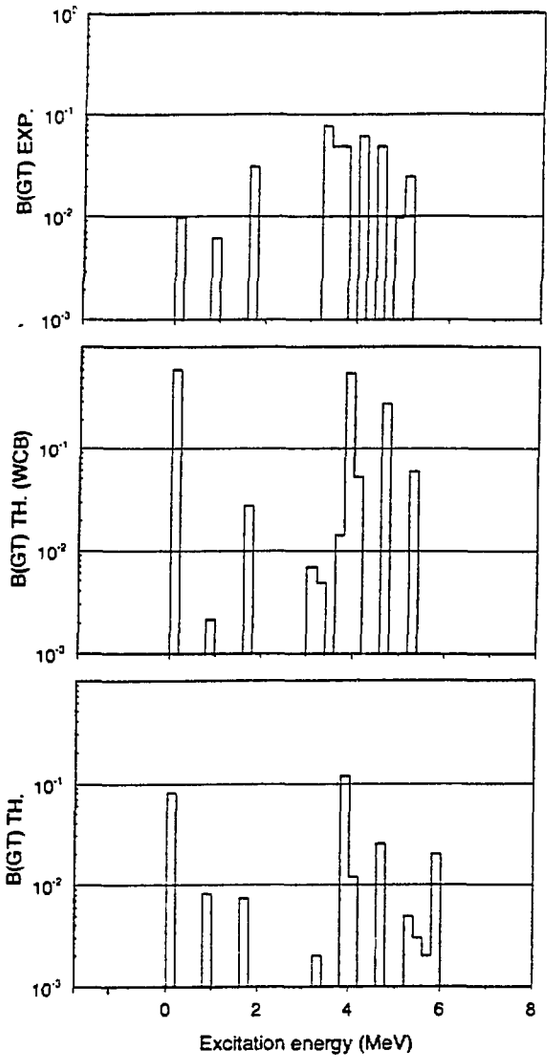

Fig.16